Pure appl. geophys. 164 (2007) 355–378
0033–4553/07/030355–24
DOI 10.1007/s00024-006-0180-5

Pure and Applied Geophysics

M_{TSU} : Recovering Seismic Moments from Tsunameter Records

EMILE A. OKAL[1] and VASILY V. TITOV[2]

Abstract—We define a new magnitude scale, M_{TSU}, allowing the quantification of the seismic moment M_0 of an earthquake based on recordings of its tsunami in the far field by ocean-bottom pressure sensors ("tsunameters") deployed in ocean basins, far from continental or island shores which are known to affect profoundly and in a nonlinear fashion the amplitude of the tsunami wave. The formula for M_{TSU}, $M_{TSU} = \log_{10} M_0 - 20 = \log_{10} X(\omega) + C_D^{TSU} + C_S^{TSU} + C_0$, where $X(\omega)$ is the spectral amplitude of the tsunami, C_D^{TSU} a distance correction and C_S^{TSU} a source correction, is directly adapted from the mantle magnitude M_m introduced for seismic surface waves by OKAL and TALANDIER. Like M_m, its corrections are fully justified theoretically based on the representation of a tsunami wave as a branch of the Earth's normal modes. Even the locking constant C_0, which may depend on the nature of the recording (surface amplitude of the tsunami or overpressure at the ocean floor) and its units, is predicted theoretically. M_{TSU} combines the power of a theoretically developed algorithm, with the robustness of a magnitude measurement that does not take into account such parameters as focal geometry and exact depth, which may not be available under operational conditions in the framework of tsunami warning. We verify the performance of the concept on simulations of the great 1946 Aleutian tsunami at two virtual gauges, and then apply the algorithm to 24 records of 7 tsunamis at DART tsunameters during the years 1994–2003. We find that M_{TSU} generally recovers the seismic moment M_0 within 0.2 logarithmic units, even under unfavorable conditions such as excessive focal depth and refraction of the tsunami wave around continental masses. Finally, we apply the algorithm to the JASON satellite trace obtained over the Bay of Bengal during the 2004 Sumatra tsunami, after transforming the trace into a time series through a simple *ad hoc* procedure. Results are surprisingly good, with most estimates of the moment being over 10^{29} dyn-cm, and thus identifying the source as an exceptionally large earthquake.

Key words: Tsunami, magnitudes, normal mode theory, tsunami warning.

Introduction

With the recent development and deployment of tsunameters under the DART project (GONZÁLEZ *et al.*, 2005), it has become possible, at least in the Pacific Ocean, to routinely record tsunami waves on the high seas, unaffected by the distortion they undergo during the complex, highly nonlinear, process of shoaling and run-up at continental and island shores. We recall that tsunameters consist of pressure sensors

[1] Department of Geological Sciences, Northwestern University, Evanston, IL 60208, USA.
[2] Pacific Marine Environmental Laboratories, NOAA, 7600 Sandpoint Way, Seattle, WA 98105, USA.

deployed on the ocean floor, capable of recording the overpressure accompanying the passage of the tsunami wave, and of relaying this information to a remote data center via satellite communication from a surface buoy which receives the signal acoustically from the nearby deep-water sensor (Fig. 1).

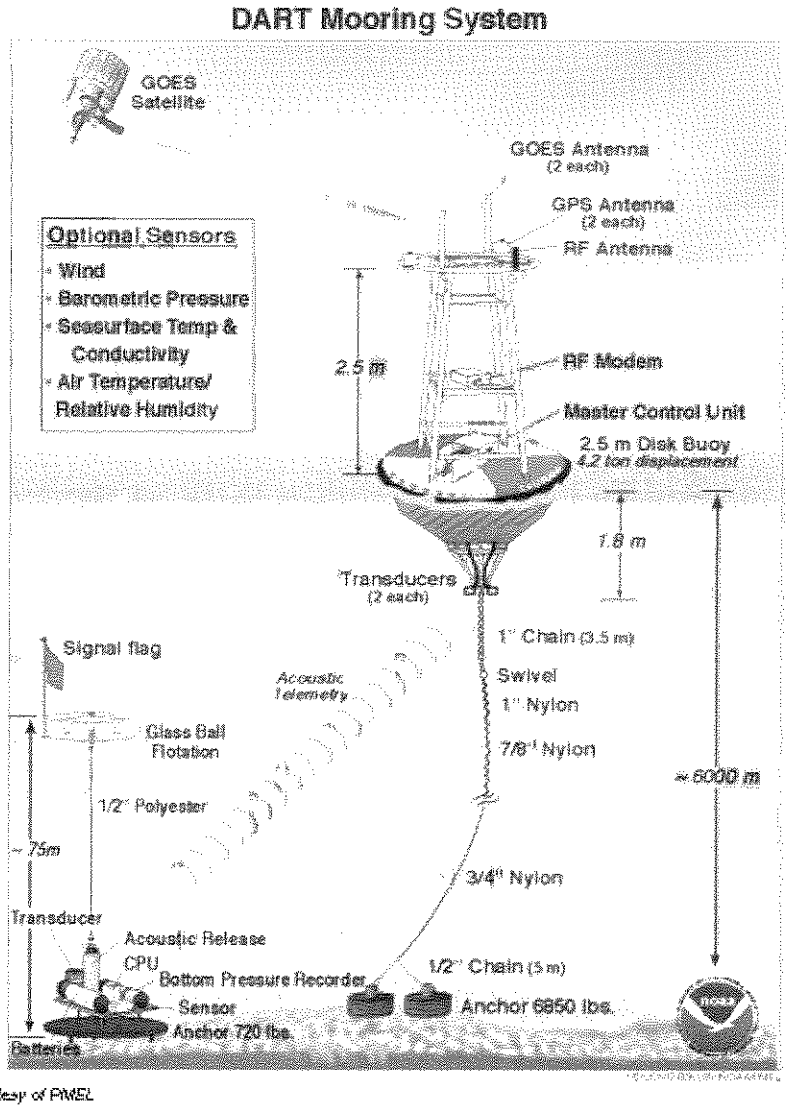

Figure 1
Schematic diagram of a DART tsunameter (GONZÁLEZ *et al.*, 2005). The pressure sensor (bottom left) is deployed on the ocean floor and its signal relayed acoustically to a buoy floating nearby, which in turn transmits the data to a central laboratory via satellite telemetry.

At least three other technologies have been used to detect tsunami waves on the high seas, some of which lend themselves to a quantitative measurement. (1) OKAL *et al.* (1999) analyzed satellite altimetry signals in the wake of several tsunamis in the 1990s, and claimed the detection of an 8-cm signal following the 1992 Nicaraguan event, and the tentative recognition of the 1995 Antofagasta, Chile tsunami. Satellite altimetry successfully detected the 2004 Sumatra tsunami, with an amplitude of 70 cm on the JASON satellite trace (SCHARROO *et al.*, 2005), which was successfully modeled by, among others, TITOV and ARCAS (2005) and SLADEN and HÉBERT (2005). (2) Following an idea originally proposed by WEAVER *et al.* (1970) and PELTIER and HINES (1976), ARTRU *et al.* (2005) used dense arrays of land-based GPS receivers to detect a disturbance in the electron density of the ionosphere, induced by the upwards continuation of the tsunami eigenfunction, first in the wake of a small earthquake south of Japan, then during the large Peruvian event of 2001. This technique also detected successfully the 2004 Sumatra tsunami (OCCHIPINTI *et al.*, 2005), leading to a preliminary quantitative interpretation in terms of an estimate of the vertical amplitude of the tsunami wave at the surface of the ocean. (3) More recently, HANSON and BOWMAN (2005) reported the detection of the 2004 Sumatra tsunami on hydrophones of the International Monitoring System. Such instruments are conceptually similar to tsunameters, in that they detect the pressure component of the tsunami wave in the oceanic water column, albeit at a different depth (1.3 km as opposed to the ocean floor for tsunameters); they also feature a drastically different instrumental response. These authors did not address the question of the amplitude of the reported signals. which OKAL *et al.* (2007) later interpreted quantitatively in the 10 mHz frequency range.

In the framework of far-field tsunami warning, signals from tsunameters can provide a crucial input to the rapid quantification of the source. In this respect, it should be possible to interpret the amplitude of tsunameter signals in terms of the lowest-frequency components of the seismic moment release. The purpose of the present paper is the development of an ultra-long period seismic magnitude scale, M_{TSU}, based on the measurement of far-field tsunami waves on the high seas. We wish to emphasize that it differs fundamentally from the "tsunami magnitude" M_t introduced by ABE (1981), which, we recall, consists of interpreting maximum tidal gauge or run-up measurements, which by definition include the effects of shoaling and the responses of coastlines, bays and harbors. Furthermore, M_t remains an empirical concept, which does not lend itself to a full theoretical justification of its algorithm, and in particular of its distance correction and locking constants. By contrast, our approach is to derive theoretically in Section 2 an algorithm for the retrieval of the seismic moment M_0 of an earthquake from a tsunameter record of its tsunami. In Section 3, we test the method on records obtained by numerical simulation, and in Section 4, we examine an actual dataset of 24 records from seven Pacific tsunami events in the years 1994–2003. We further illustrate that the concept may be applied to satellite altimetry by

processing the JASON trace recorded over the Bay of Bengal during the 2004 Sumatra tsunami.

2. Theory

Our theoretical approach for the development of M_{TSU} closely follows that of the mantle magnitude M_m introduced by OKAL and TALANDIER (1989). We recall that the M_m algorithm consists of measuring the spectral amplitude $X(\omega)$ of long-period Rayleigh or Love mantle waves, and of calculating an estimate of the seismic moment M_0 of the source as

$$M_m = \log_{10} M_0 - 20 = \log_{10} X(\omega) + C_D + C_S + C_0. \quad (1)$$

In this formula, M_0 is in dyn*cm, $X(\omega)$ is expressed in μm*s, and the distance and source corrections, C_D and C_S, as well as the locking constant C_0, are all derived theoretically from normal mode theory, under the surface wave asymptotic approximation. As detailed in OKAL and TALANDIER (1989), the power of the mantle magnitude algorithm resides in that it combines the practicality of the magnitude approach (a "quick-and-dirty" measurement ignoring details of focal mechanism geometry and exact source depth), with a modern theoretical approach, *i.e.*, the measurement of a *bona fide* physical quantity, namely the seismic moment M_0, in the framework of an established physical theory. Finally, because it uses a variable frequency, M_m does not saturate, as do conventional magnitude scales (GELLER, 1976), even for the largest earthquakes ever recorded, such as the 1960 Chilean event (OKAL and TALANDIER, 1991).

We refer to the series of seminal papers by WARD (1980; 1981; 1982a,b), in which he describes tsunami waves as a particular branch of the spheroidal family of normal modes of the Earth. The power of this approach is that the analytical formalism developed for example by ALTERMAN *et al.* (1959) (actually traceable to LOVE's (1911) famous monograph) for the computation of the eigenfunctions of the Earth's modes is directly applicable to the case of tsunamis, as long as the Earth model includes an oceanic layer and the computation is carried out in the full six-dimensional space allowing for the effect of gravity. This includes the computation of the excitation of an individual mode by a double-couple source located in the solid Earth (SAITO, 1967; GILBERT, 1970), for which the expression of the excitation coefficients (K_0, K_1, K_2 in the notation of KANAMORI and CIPAR 1974) can be directly transcribed to the case of the tsunami eigenfunction. As discussed by OKAL (1982; 1988; 1990), this allows the direct and seamless handling of the coupling between the ocean water layer and any vertically heterogeneous solid Earth structure, including sedimentary layers. In particular, the normal mode approach does not make any assumptions on the parameter kH scaling the equivalent wavelength $2\pi/k$ to the depth of the ocean column H, and as such remains applicable outside the range of the shallow-water approximation.

However, normal mode theory is by nature linear and also requires, at least in the simpler application considered here, a spherically symmetric structure involving an ocean covering the entire planet with a uniform depth H, which we will take as 5 km. While these approximations may seem drastic, the robustness of the concept of magnitude for seismic waves (and normal modes, including tsunamis) is such that they do not significantly limit the applicability of our algorithm, as detailed below in Sections 3 and 4.

Accordingly, the spectral amplitude $X(\omega)$ of the vertical displacement $\eta(t)$ of the tsunami wave generated by a double-couple of moment M_0 at an epicentral distance Δ is given by the same formula as that of a Rayleigh wave

$$X(\omega) = M_0 \cdot a\sqrt{\frac{\pi}{2}} \cdot \frac{1}{\sqrt{\sin\Delta}} \cdot \left[\frac{1}{U}\left|s_R l^{-1/2} K_0 - p_R l^{3/2} K_2 - i q_R l^{1/2} K_1\right|\right], \tag{2}$$

so that in turn M_{TSU} will be given by a formula similar to (1)

$$M_{TSU} = \log_{10} M_0 - 20 = \log_{10} X(\omega) + C_D^{TSU} + C_S^{TSU} + C_0. \tag{3}$$

In these formulæ, a is the radius of the Earth, l the orbital number of the spheroidal mode, related to the equivalent wavenumber through $l = ka - 1/2$, U is the group velocity of the wave at angular frequency ω, the excitation coefficients K_i depend only on frequency and depth (KANAMORI and CIPAR, 1974), and the trigonometric coefficients s_R, p_R and q_R depend only on focal geometry and receiver azimuth.

- In (2), we have neglected any non-geometric attenuation of the wave, so that the new distance correction is simply

$$C_D^{TSU} = \frac{1}{2}\log_{10}\sin\Delta. \tag{4}$$

- As the locking constant C_0 simply compensates for the term $a \cdot \sqrt{\pi/2}$, it will take the same value as in the case of Rayleigh waves, $C_0 = 3.10$ if $X(\omega)$ is expressed in cm*s and all computations are carried out with traditional units, *i.e.*, the K_i's are in 10^{-27} dyn^{-1} and U in km/s. ($C_0 = -0.90$ if $X(\omega)$ is in μm*s.)
- The source correction C_S^{TSU} is designed to correct for the term in large brackets in (2), $E(\phi_f, \delta, \lambda; \phi_s; h; \omega)$, under the formalism of a magnitude measurement, *i.e.*, for average focal mechanism geometry (defined by the three angles ϕ_f, δ, λ), receiver azimuth ϕ_s, and source depth h. Following OKAL and TALANDIER (1989), we derive an expression of C_S^{TSU} by looping, for each source depth h, over a very large number N of focal geometries, and computing the logarithmic average excitability

$$L_{av} = \log_{10} E_{av}(h, \omega) = \log_{10}\left[\frac{1}{N}\sum_{\delta,\lambda;\phi} E(\phi_f, \delta, \lambda; \phi_s; h; \omega)\right], \tag{5}$$

using the actual excitation coefficients computed from normal mode solutions. Figure 2 shows the results of these computations for $N = 49248$ source-receiver geometries and 10 source depths, from $h = 6$ km (1 km below the ocean floor; symbols "0") to 100 km (symbols "9"). It is equivalent to Figure 3 of OKAL and TALANDIER (1989). Note that, except for the greatest depths (80 km, "8"; and 100 km, "9"), the excitability features little dependence on depth at periods greater than 600 s, typical of far-field tsunamis generated by very large earthquakes, as predicted by WARD (1981) and OKAL (1988). As expected, at shorter periods, depth starts to play a role for increasingly shallow sources.

At each period, we average L_{av} obtained from (5) over those depths for which L_{av} remains in the pack (all depths for $T > 1000$ s; eliminating 100 km under 1000 s, 80 and 100 km under 820 s; etc. up to keeping only $h \leq 20$ km under 300 s). The resulting averages are plotted as the solid dots on Figure 2. We then regress these values using a cubic spline, as in OKAL and TALANDIER (1989). The result is

$$\langle L_{av} \rangle = -0.84526\,\theta^3 - 0.53189\,\theta^2 - 0.55748\,\theta - 2.2974, \tag{6}$$

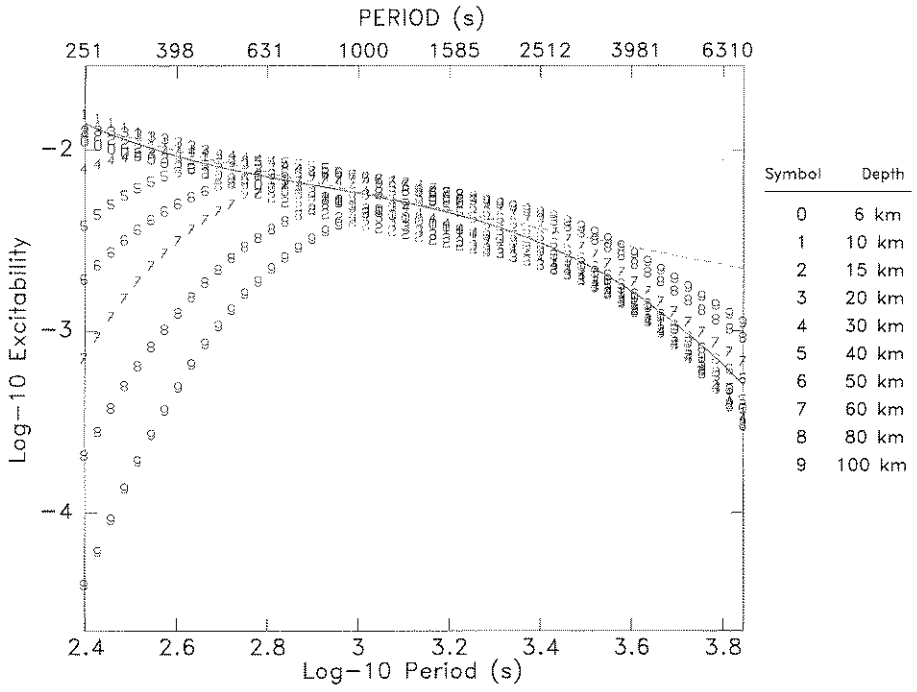

Figure 2

Logarithmic average excitability L_{av} as a function of period T. At each depth h, L_{av} is computed from (5), and the results plotted using symbols "0" ($h = 6$ km) to "9" ($h = 100$ km). The solid dots are average values of L_{av} (see text for details), and the solid line their regression by a cubic spline (6). The dashed line is the excitability predicted by (10), using the asymptotic theory.

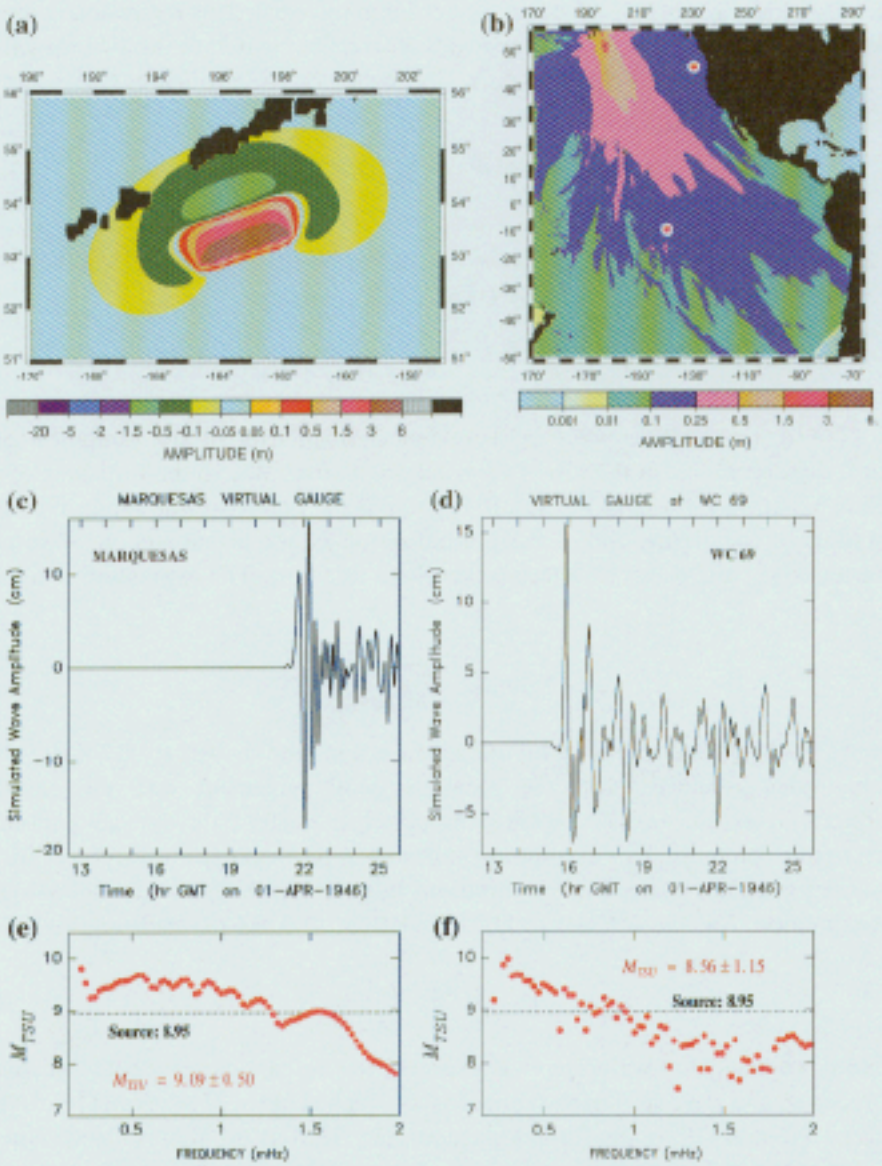

Figure 3

Test of the M_{TSU} concept and algorithm on a simulation of the 1946 Aleutian earthquake. (*a*): Static displacement field of the source area used as an initial condition of the simulation. (*b*): Maximum sea-surface height obtained by simulating the first 18 hours of propagation in the Pacific Basin. Note the strong directivity in the resulting field of amplitudes. The two bull's eye symbols represent the virtual gauges at WC69 (next to the North American Coast) and in the Marquesas. (*c*) and (*d*): Synthetic sea-surface time series at the virtual gauges. The origin of the time axis is the source time of the earthquake, 12:29 GMT on 01 April, 1946. The results of applying the M_{TSU} algorithm to these records are given in (*e*) (Marquesas) and (*f*) (WC69), and compared to the source value used in the synthetics (*dashed lines*).

where $\theta = \log_{10} T - 3.1215$ (T being the period in seconds). This regression is shown as the solid curve on Figure 2, and provides an excellent match to the average values of L_{av}, as defined by the individual dots. Consequently, the correction C_S^{TSU} can be taken as

$$C_S^{TSU} = -\langle L_{av} \rangle = 0.84526\,\theta^3 + 0.53189\,\theta^2 + 0.55748\,\theta + 2.2974 \quad (\theta = \log_{10} T - 3.1215) \tag{7}$$

We also verified that this formula is well predicted by the asymptotic expressions of the excitation coefficients defined by OKAL (2003), namely

$$K_2 = \frac{1}{8\pi\mu}\frac{Y^{-1}}{la^2}; \quad K_0 = l(l+1)K_2; \tag{8}$$

and $K_1 = 0$, the latter expressing the classical singularity of the excitation of a vertical dip-slip source at the top of the solid Earth, itself due to the vanishing of the traction $\sigma_{r\theta}$ at the bottom of the ocean. In (8), μ is the rigidity of the source region, a the radius of the Earth, and Y the normalization of the eigenfunction of vertical displacement at the ocean's surface (taken here as 1 cm). The expression predicted for L_{av}

$$L_{av} = \log_{10}\left[\frac{\langle |s_R - p_R| \rangle l^{1/2}}{8\pi\mu a^2 U}\right] \tag{9}$$

is shown as the dashed curve on Figure 2, where a mantle rigidity ($\mu = 7 \times 10^{11}$ dyn/cm^2)has been assumed. Note the generally good agreement with the previous computation, except for $T > 3000$ s, in principle beyond the typical period of transoceanic tsunamis. This asymptotic approach is particularly powerful, because it allows in principle a correction for variations in water depth H. In the shallow water approximation, $l = a\omega/C$, $C = (g\,H)^{1/2}$, and $U = C$. Then (9) leads to

$$C_S^{TSU} = -L_{av} = -\log_{10}\left[\frac{\langle |s_R - p_R| \rangle \omega^{1/2} g^{-3/4}}{8\pi\mu a^{3/2}} \cdot H^{-3/4}\right]. \tag{10}$$

Note, however that water depth is expected to vary significantly between source and receiver, and the question then arises as to which value of H to use in (10). In this respect, the normal mode formalism does not lend itself well to such lateral heterogeneities in structure; nevertheless, we can make the following argument: at any given angular frequency ω, the propagation terms of the Fourier integral under the asymptotic approximation of the Legendre polynomials in (2) will involve the average water depth along the path, H_p. These terms are proportional to $l^{-1/2}/U$ for the isotropic $m = 0$ term in (2), which will behave like $H_p^{-1/4}$ under the shallow-water approximation. For the clover-leaf $m = 2$ term, $l^{3/2}/U$ will behave like $H_p^{-5/4}$. By contrast, the expression of the excitation coefficients K_0 and K_2 will be controlled by the water depth at the source, H_s, with according to (8), $K_2 \sim l^{-1} \sim H_s^{1/2}$ and

$K_0 \sim l \sim H_s^{-1/2}$. Thus the term $H^{-3/4}$ in (10) should be split as $H_p^{-1/4} H_s^{-1/2}$ for the isotropic $m = 0$ terms and $H_p^{-5/4} H_s^{1/2}$ for the clover-leaf $m = 2$ ones.

Thus, one would expect that any difference between H_p and H_s would act in opposite ways on the two terms, suggesting an overall trade off. In addition, the situation will be made even more complex by the fact that a source water depth H_s will be difficult to define, as the source region of most large tsunamis in subduction zones (integrated over the full extent of the fault width in the rupture area) is bound to feature significant variations in bathymetry, in the presence of the trench–arc system.

In the context of a magnitude scale, characterized by measurements necessarily averaged over a large number of parameters and by a logarithmic scale, it appears justified to remain with an average estimate H in (10). In principle, one could further define a water depth correction to be added to (10) or (7):

$$C_{WD} = \frac{3}{4} \log_{10} \left[\frac{H}{H_{5000}} \right], \tag{11}$$

where $H_{5000} = 5000$ m, and H would be an appropriate measure of the average water depth at the source and along the path to the receiver. We note however that, for long transoceanic paths, H will rarely be less than 3000 m, leading to a correction of less than 0.2 units of M_{TSU}, which we regard as negligible in view of the many other approximations made.

Next, we note that tsunameters record the overpressure at the bottom of the ocean, $p(t)$, rather than the displacement at the surface, $\eta(t)$, the relation between the two being simply (OKAL, 1982)

$$p(t) = \rho_w g \eta(t) \quad \text{or} \quad P(\omega) = \rho_w g X(\omega), \tag{12}$$

where ρ_w is the density of water (1 g/cm^3) and g the acceleration of gravity (981 cm/s^2). We can then rewrite (3) as

$$M_{TSU} = \log_{10} P(\omega) + C_D^{TSU} + C_S^{TSU} + C_0^P, \tag{13}$$

where the new locking constant is simply $C_0{}^P = C_0 - \log_{10}(\rho_w g) = 3.10 - 2.99 = 0.11$ if p is measured in dyn/cm^2 (also called "baryes"), and hence $P(\omega)$ in barye*s, which is the cgs unit of kinematic viscosity, called a "poise".

NOAA sensors of the DART program actually output p in British units, reportedly pounds per square inch, or "psi". These should actually be called "pounds–*force* per square inch" (pfsi) to be appropriate units of pressure. The relationship of pfsi to baryes involves the acceleration of gravity (going from psi to pfsi), and is

$$1 \text{ pfsi} = 981 \cdot \frac{453}{2.54^2} \text{ baryes} = 68881 \text{ baryes} = 10^{4.84} \text{ baryes}. \tag{14}$$

Accordingly, if p is measured in pfsi, and hence $P(\omega)$ in pfsi*s, then $C_0^P = 4.84 + 0.11 = 4.95$ in (13).

In summary, the algorithm of M_{TSU} proceeds as follows: Given a time series of overpressure measurements at the bottom of the ocean, obtain its spectral amplitude $P(\omega)$ at all periods between 600 and 3500 seconds, apply the distance and source corrections C_D^{TSU} (4) and C_S^{TSU} (7), and use the appropriate locking constant C_0^P depending on recording units. Then the quantity (13) should be an approximation of $\log_{10} M_0$–20, where M_0 is in dyn*cm. M_{TSU} can also be related to the so-called "moment magnitude" introduced by KANAMORI (1977) through $M_{TSU} = 1.5\, M_w$–3.9.

3. Validation on Numerical Simulations

Before applying the concept of M_{TSU} to actual data recorded on tsunameters, we proceed to validate the algorithm on synthetic data obtained by hydrodynamic simulation of the far-field tsunami of a very large earthquake. For this purpose, we use the geometry of the 1946 Aleutian tsunami, with a model inspired by the work of LÓPEZ and OKAL (2006), and featuring a seismic moment $M_0 = 9 \times 10^{28}$ dyn-cm, with a bilateral rupture totaling 200 km, and a slip reaching 10 m. This source was used successfully by OKAL and HÉBERT (2007) to model a dataset of 27 run-up values obtained in the far field by OKAL *et al.* (2002). The static displacement created by the earthquake source in the epicentral area was computed using MANSINHA and SMYLIE'S (1971) algorithm, and is shown in Figure 3*a*. It forms the initial condition of a simulation using the MOST code (TITOV and SYNOLAKIS, 1998), which solves the nonlinear equations of hydrodynamics, depth-averaged under the shallow water approximation, using a finite-difference algorithm and the method of splitting integration steps. Details are provided in SYNOLAKIS (2002). We compute virtual gauge records at two locations, one at a DART site WC69 off the coast of Oregon (45.933°N, 129.981°W; 2486 km from the source), and the other off the Marquesas Islands (9°S, 140°W; 7246 km from the source). Figure 3*b* shows that the former is located outside the main lobe of directivity of the tsunami wave, oriented perpendicular to the direction of rupture as predicted by BEN-MENAHEM and ROSENMAN (1972). As the algorithm for M_{TSU}, based on the concept of magnitude, ignores directivity, it is important to test its effect on the final result.

Figures 3c and 3d show time series of the simulated tide gauges at the two locations. The Marquesas record has a greater peak-to-peak amplitude, and is obviously richer in high frequencies, than its counterpart at WC69, even though it is located at greater distance; this illustrates the effect of source directivity. The time series were then processed through the M_{TSU} algorithms, using Equation (3). The results are shown on the bottom frames (Figs. 3e and 3f), where the dots represent individual M_{TSU} measurements and the dashed line the value (8.95) corresponding to

the seismic moment used. The agreement is generally good, and clearly better at the Marquesas receiver, located in the lobe of directivity than at the West Coast one, which suffers from destructive interference at frequencies above 1 mHz. Nevertheless, the algorithm still recovers an appropriate value of M_0 from the WC69 synthetic, using the lower frequencies (0.5–1.2 mHz).

4. Application to Real Data

The algorithm M_{TSU} was then applied to the case of seven Pacific Ocean tsunamis recorded by DART stations in the far field during the years 1994–2003. Tables 1 and 2 lists all relevant details of the experiment.

• *Event 1; Kurile Islands, 04 OCT 1994*

Figure 4 presents details of the methodology applied to all records, in the case of the 1994 Kurile Island tsunami, which was locally destructive in the Southern Kurile Islands (YEH *et al.*, 1995). This event was recorded by four tsunameters (AK 59 and 60 off the Alaskan Peninsula, and WC 61 and 62 off the West Coast of the US); note the coherence of signals at nearby locations. However, despite featuring the largest seismic moment of any event recorded by DART to date ($M_0 = 3 \times 10^{28}$ dyn*cm), the earthquake does not constitute an interplate thrust event, but rather a probable tear within the subducted lithosphere (TANIOKA *et al.*, 1995). As such, its depth (68 km) and focal mechanism (shown in Fig. 4*a*) are unfavorable to the generation of a distant tsunami, especially in the azimuth of the available tsunameters.

For each tsunameter signal, we define a 12-hour window, and simply apply (3) to its Fourier spectrum, within ranges of frequencies offering suitable signal-to-noise ratios, as defined by comparing with the spectra of similar windows on the preceding day (Fig. 4*c*). The results in Table 1 show that the two West Coast stations give values (8.23 $\pm$ 0.37 and 8.25 $\pm$ 0.39) compatible with the expected value (8.48), if slightly underestimating it, whereas the Gulf of Alaska records are somewhat deficient (7.98 $\pm$ 0.24 and 7.95 $\pm$ 0.31). This is probably due to the unfavorable geometry of the relevant paths, the great circle to the AK sites crossing substantially into the Bering Sea (Fig. 4*a*), in particular through its shallow eastern half, which consists of an extended continental shelf. By contrast, the West Coast records are apparently less affected by the passage of the great circle over the Aleutians; it is probable that the actual ray paths are slightly refracted around the arc. It remains remarkable that the moment of the earthquake is well recovered, within the error bars of the WC measurements, despite unfavorable centroid depth (68 km) and station azimuth for the particular mechanism involved.

Table 1

M_{TSU} measurements for seven Pacific tsunamigenic earthquakes, 1994–2003

Event Number and Region	Station	Date	Origin	CMT Solution			M_{TSU}	
		D M (J) Y	Time (GMT)	Lat.; Lon. (°N; °E)	Depth (km)	Moment (10^{27} dyn*cm)	predicted	measured
1. Kurile Is.		04 OCT (277) 1994	13:23	43.6; 147.6	68	30	8.48	
	AK 59							7.98 ± 0.24
	AK 60							7.95 ± 0.31
	WC 61							8.25 ± 0.39
	WC 62							8.23 ± 0.37
	Average							**8.08 ± 0.14**
2. Kurile Is.		03 DEC (337) 1995	18:01	44.82; 150.17	26	8.24	7.92	
	AK 64							7.58 ± 0.35
	WC 67							7.87 ± 0.28
	WC 68							7.89 ± 0.25
	WC 69							7.88 ± 0.24
	Average							**7.81 ± 0.13**
3. Andreanof Is.		10 JUN (162) 1996	04:04	51.10; −177.41	29	8.05	7.91	
	WC 67							7.84 ± 0.22
	WC 68							7.86 ± 0.21
	WC 69							7.75 ± 0.26
	Average							**7.82 ± 0.05**
4. Biak		17 FEB (048) 1996	06:00	−0.67; 136.62	15	24.1	8.38	
	AK 64							8.13 ± 0.28
	WC 67							8.29 ± 0.30
	WC 68							8.39 ± 0.24
	WC 69							8.32 ± 0.28
	Average							**8.28 ± 0.10**
5. No. Chile		30 JUL (211) 1995	05:11	−24.17; −70.74	29	12.1	8.08	
	AK 64							8.08 ± 0.26
	WC 67							8.00 ± 0.31
	WC 68							8.08 ± 0.24
	WC 69							8.04 ± 0.25
	Average							**8.05 ± 0.03**
6. Mexico		09 OCT (282) 1995	15:36	19.34; −104.80	15	11.5	8.06	
	AK 64							7.50 ± 0.29
	WC 67							7.86 ± 0.29
	WC 68							7.92 ± 0.24
	WC 69							8.00 ± 0.20
	Average							**7.82 ± 0.19**
7. Aleutian Is.		17 NOV (321) 2003	06:43	51.14; 177.86	22	5.3	7.71	
	D171							**7.70 ± 0.22**

Table 2

Tsunameters used in this study

Code	Region	Latitude °N	Longitude °E	Water depth (m)	Event(s) recorded
AK 59	Gulf of Alaska	54.044	−158.749	5889	1
AK 60	Gulf of Alaska	54.022	−155.729	4553	1
AK 64	Gulf of Alaska	53.430	−157.290	4550	2,4,5,6
WC 61	Off West Coast of U.S.	45.960	−129.964	2420	1
WC 62	Off West Coast of U.S.	45.953	−129.999	2440	1
WC 67	Off West Coast of U.S.	45.960	−129.970	2420	2,3,4,5,6
WC 68	Off West Coast of U.S.	45.960	−130.000	2435	2,3,4,5,6
WC 69	Off West Coast of U.S.	45.933	−129.981	2447	2,3,4,5,6
D 171	Off Aleutian Islands	46.630	−170.790	5654	7

• *Event 2; Kurile Islands, 03 DEC 1995*

The situation is very similar in the case of the smaller Kurile Islands event of 03 December, 1995, which occurred about 250 km to the northeast, but was a *bona fide* interplate thrust event at a regular depth (26 km). As shown in Figure 5 (top panels), the three West Coast stations recover the earthquake's moment flawlessly, while Receiver AK64 remains deficient, probably again on account of the incursion of the path into the Bering Sea. The comparison with Event 2 shows that the variations in depth (as long as the source remains shallower than 60 km) and focal mechanism do not affect significantly the relationship between earthquake moment and far-field tsunami amplitude on the high seas. Even though this observation may seem paradoxical, it is in general agreement with the results of WARD (1981) and OKAL (1988); this justifies *a posteriori* the use a magnitude concept in which such details are ignored.

• *Event 3; Andreanof Islands, 10 JUN 1996*

The tsunami was recorded only at the West Coast sites, as the Gulf of Alaska tsunameters were not operational at the time. As shown on the central panels of Figure 5, the M_{TSU} algorithm recovers the seismic moment of the event adequately at all three sites.

• *Event 4; Biak (Indonesia), 17 FEB 1996*

For this large earthquake in the Western Equatorial Pacific, great circle paths to both the Alaskan and West Coast locations should be unaffected by the Aleutian arc, and all four records yield adequate values of the moment, even though Station AK 64 still provides the lowest value (Fig. 5; lower panels).

• *Event 5; Antofagasta, Chile, 30 JUL 1995*

This earthquake generated a significant tsunami in the South Pacific, which knocked a supply ship to the bottom of the harbor at Ua Pou, in the Marquesas

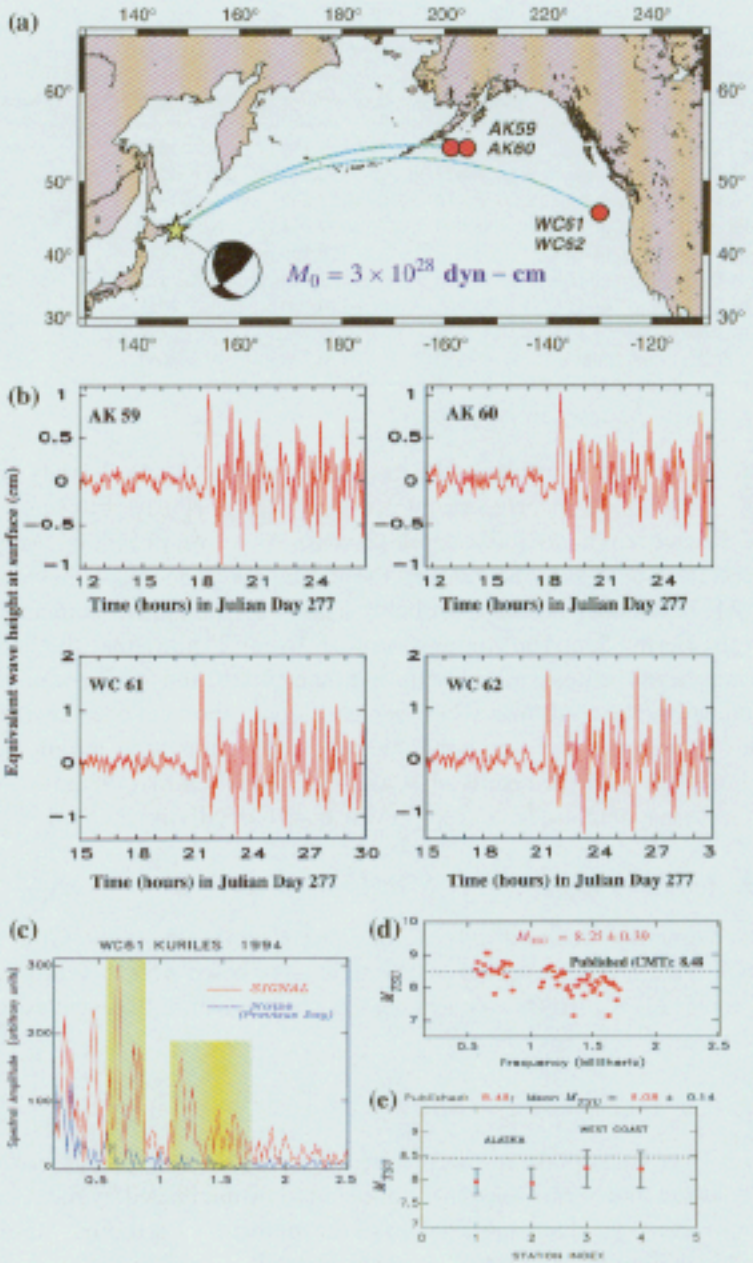

Islands (GUIBOURG *et al.*, 1997). We tested the algorithm in the case of this large earthquake, even though the geometry of the great circle paths from its source to the tsunameters involves significant land paths (Fig. 6a). This should in principle

Figure 4
Computation of M_{TSU} for the 1994 Kuriles earthquake. (*a*): Map of the Northern Pacific showing the location of the source (*star*) and receivers (*solid dots*). Note that the great circle paths to the tsunameters intersect the Aleutian chain. (*b*): Original records at the four tsunameter sites. The vertical axis has been converted to equivalent surface amplitude, using (12). Note the remarkable signal coherence at nearby sites AK59 and 60 and at WC61 and 62. (*c*): Optimization of frequency windows based on signal-to-noise ratios, illustrated on the WC61 record. Based on a comparison with spectra for the previous day, the two shaded frequency bands (in this case 0.55–0.86 mHz and 1.06–1.71 mHz) are retained in the computation. (*d*): Individual M_{TSU} values (*solid dots*) computed inside the frequency bands, compared with the published value derived from the CMT solution (*dashed line*). (*e*): Summary of results for the four tsunameters.

invalidate the use of the M_{TSU} algorithm, since WARD's (1980) formalism, on which Equation (2) is based, is valid only for a laterally homogeneous ocean basin. Yet, the vigor of the signals recorded at all sites clearly indicates refraction around the coasts of Central and North America, and, remarkably, all four values of M_{TSU} recover the seismic moment perfectly (Fig. 6*b*). Once again, this expresses the robustness of the concept of magnitude, which manages to override the nongeometrical propagation, which apparently affects only marginally the spectral amplitudes of the waves as recorded in the Northeastern Pacific.

• *Event 6; Mexico, 09 OCT 1995*

Bolstered by the Chilean results, we decided to process the tsunameter records of this large event, for which the great circles to the tsunameters similarly interfere with land masses over a large portion of their paths (Fig. 6c). The results are surprisingly good at the West Coast stations, but show a significant deficiency at the Gulf of Alaska instrument (Fig. 6d).

• *Event 7; Aleutian Islands, 17 NOV 2003*

This considerably smaller event ($M_0 = 5.2 \times 10^{27}$ dyn-cm) did not generate a tsunami in the far field and was not recorded above noise level on the tsunameters in the Gulf of Alaska and along the West Coast of the U.S. It was, however, recorded with an equivalent surface amplitude of 4 cm peak-to-peak by a newly installed instrument, D-171, only 900 km from the epicenter (Figs. 7a, b). The good agreement between M_{TSU} and the published CMT moment (Fig. 7d) illustrates the feasibility of using the algorithm in the regional field ($\Delta \approx 1000$ km), in particular in the case of smaller events whose tsunamis may not be detectable in the far field. On the other hand, the absence of detectable signals in the far field suggests a lower bound of at least $M_0 \geq 6 \times 10^{27}$ dyn-cm for the method to be applicable. This estimate is confirmed by the absence of a usable signal during the Chimbote, Peru tsunami earthquake of 21 February 1996 ($M_0 = 2.2 \times 10^{27}$ dyn-cm).

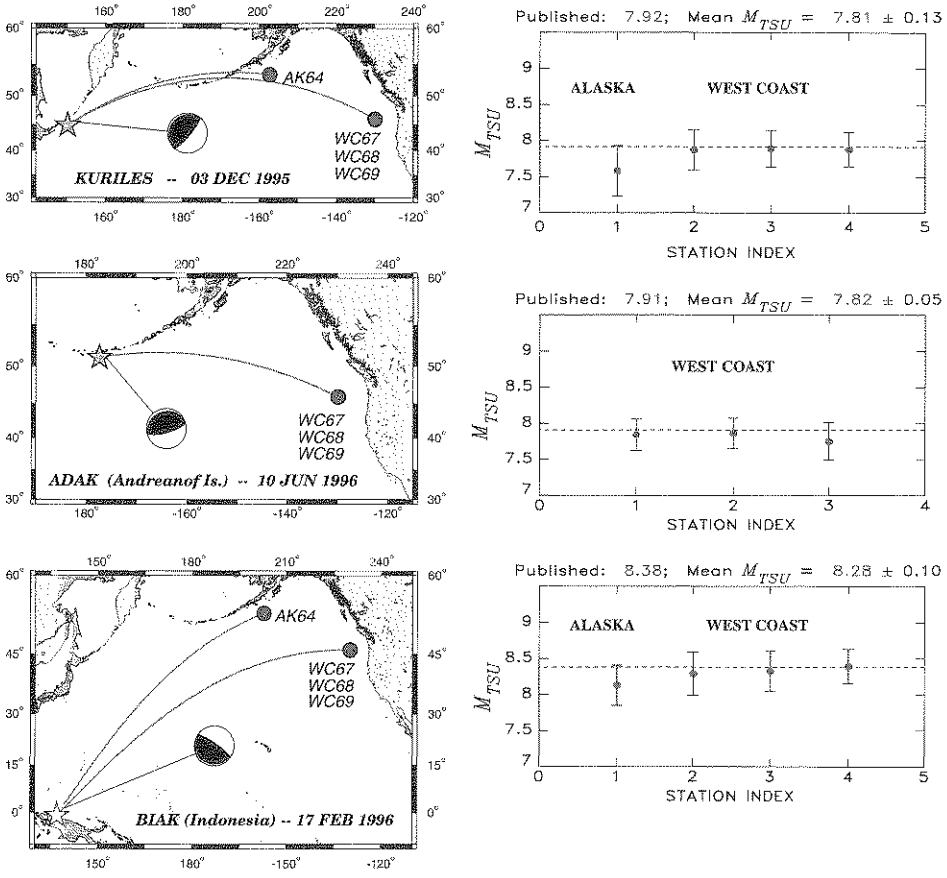

Figure 5
Results for events 2, 3, 4. Situation maps similar to Figure 4a are at *left* and summaries similar to Figure 4e at *right*. Note the generally excellent performance of the West Coast stations, but the remaining deficiency of the Gulf of Alaska tsunameter AK64.

Incidentally, the tsunameter record in Figure 7b was used in real time to estimate the moment of the event, by comparing its amplitude to those in a library of synthetic sea-surface height time series obtained by numerical simulation for a large number of earthquake scenarios along the subduction zones of the Pacific Basin (TITOV *et al.*, 2005). The estimated source was then used to forecast expected tsunami heights, notably in the Hawaiian Islands, which were found not to exceed 25 cm.

While this episode did not specifically use the M_{TSU} algorithm, it shares its philosophy and basic concept, and underlines the potential of the algorithm in the context of real-time tsunami warning.

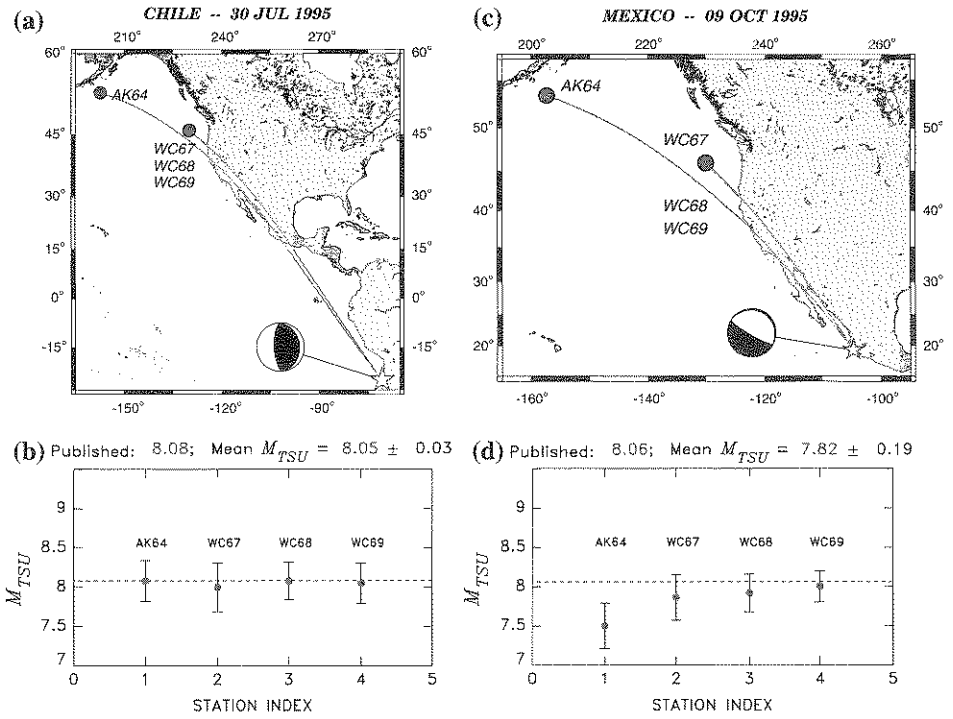

Figure 6
Results for events 5 (*a* and *b*) and 6 (*c* and *d*). In both instances, the great circle paths to the tsunameters intersect the Central and North American continental masses.

5. The Case of the JASON Trace

The catastrophic tsunami of 26 December 2004 in Sumatra was not recorded by tsunameters, since no such instruments were available in the Indian Ocean. However, there exist a number of direct observations of the deformation of the ocean surface under the passage of the tsunami from satellite altimetry traces (SCHARROO *et al.*, 2005; SLADEN and HÉBERT, 2005). We concentrate here on the so-called JASON trace, whose raw data are plotted in Figure 8b, and use it for a preliminary measurement of M_{TSU}.

As pointed out by OKAL *et al.* (1999), the interpretation of such profiles is made complex by the fact that they are neither time series (a record of the wave as a function of time at a fixed receiver), nor space series (a snapshot of the wave along a trace at a given time), because of the finite velocity of the satellite over the study area. In order to convert the JASON trace to a time series usable by the M_{TSU} algorithm, we proceed as follows: Each point i in the JASON trace, for which the sea height is η_i, corresponds to a particular position $P_i = [Lat_i; Lon_i]$ and time t_i. We correct the time

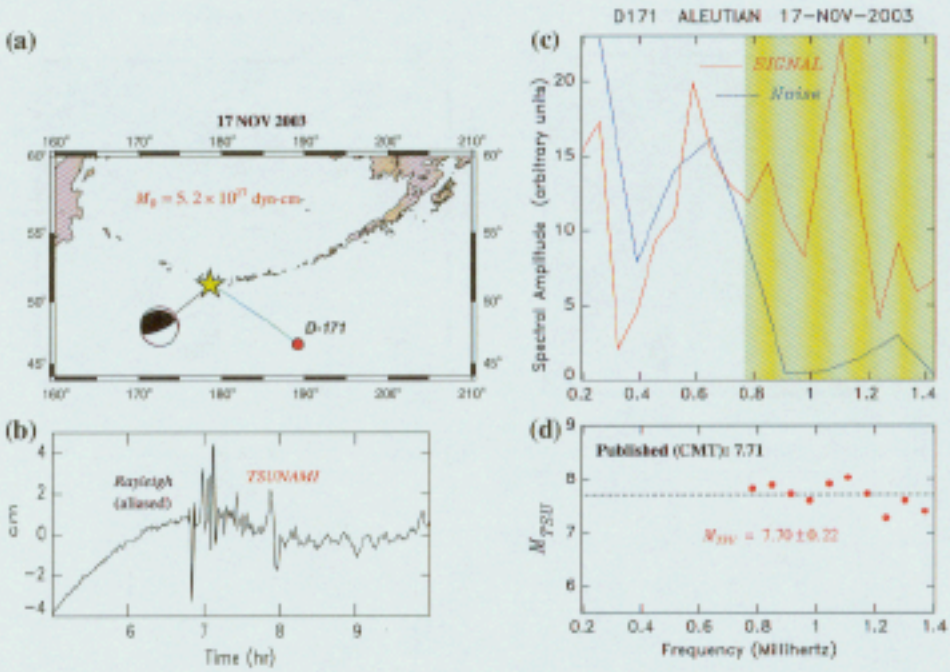

Figure 7

Case of the smaller Aleutian event of 17 November, 2003. (*a*): Location map of the epicenter and D-171 tsunameter. (*b*): Original tsunameter record at D-171. (*c*): Spectral amplitude of (*b*) defining adequate signal-to-noise ratios between 0.8 and 1.4 mHz. (*d*): Results of processing of (*b*) through the M_{TSU} algorithm, showing excellent agreement with the CMT moment.

t_i by the group time from the epicenter to P_i, assuming propagation at a constant velocity $U = 200$ m/s, to obtain

$$\tau_i = t_i - t_0 - \frac{\Delta_i}{U}, \tag{15}$$

where Δ_i is the distance separating P_i from the epicenter and t_0 the origin time of the event. Then τ_i (which can be negative) represents the time elapsed at P_i since the arrival of the first wave. We then interpret the set of η_i values as representative of the sea surface deformation at the resulting times τ_i for an average point P that we take as the location registering the maximum value of η (−3.01°N; 84.68°E). We consider only the initial part of the JASON trace, for which Δ decreases monotonically along the trace to the point of closest approach of the epicenter by the satellite. The series η_i are then re-interpolated at constant spacing $\delta\tau = 1$ s. The resulting time series is plotted on Figure 8c.

Additional approximations consist of using a point source rather than the true extent of some 1200 km of the Sumatra earthquake rupture, and of placing it at the

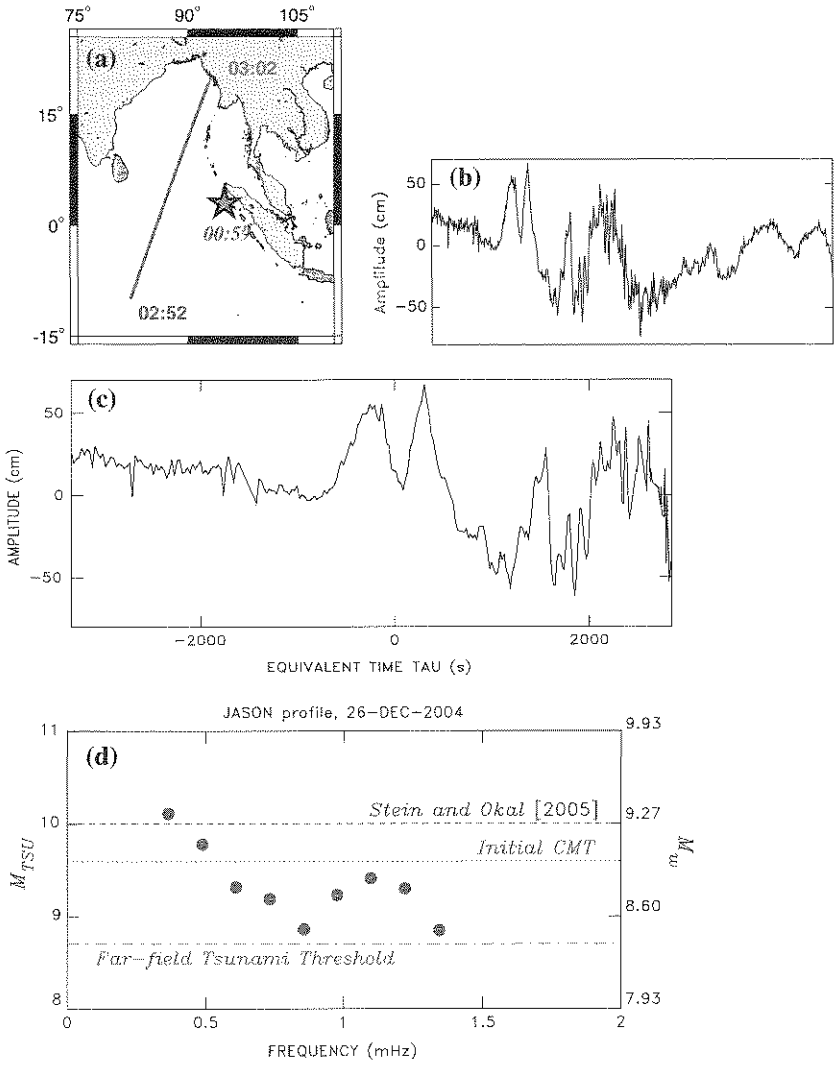

Figure 8

Processing of the JASON trace. (*a*): Map of the Bay of Bengal, showing the epicenter of the Sumatra earthquake (*star*), and the track of JASON. The satellite crosses the area from SSW to NNE approximately two hours after the occurrence of the main shock. Times at the source and at the extremities of the track are in GMT. (*b*): Original trace of sea-surface height along JASON. Both time and space vary along the abscissa. (*c*): Equivalent time series reconstructed from (b); see text for details. (*d*): Computation of M_{TSU} from the JASON profile and comparison with the initial CMT inversion (*dotted line*), the definitive moment inverted from normal modes by STEIN and OKAL (2005) (*dashed line*), and the *ad hoc* threshold for far field tsunami risk (dash-dot line).

epicenter of the earthquake (3°N; 95°E) rather than at the centroid of rupture. We justify this approach in the context of the potential future use of satellite altimetry in real-time under operational conditions where only initial determinations of the source parameters are available. We have independently verified that moving the source to the centroid of the rupture (around 7°N; 93°E) only affects the second decimal point of the values of M_{TSU}.

The time series on Figure 8c was then run through the M_{TSU} algorithm with results shown in Figure 8d, where they are compared both with the initial CMT inversion ($M_0 = 3.95 \times 10^{29}$ dyn-cm), and with the more definitive moment obtained by STEIN and OKAL (2005) from the modeling of the Earth's gravest normal modes (1.0×10^{30} dyn-cm), the latter value being also in agreement with the composite CMT inversion later proposed by TSAI *et al.* (2005). While the M_{TSU} values are relatively scattered with a mean of $M_{TSU} = 9.34 \pm 0.38$, it is remarkable that the values at the lowest frequencies (0.5 mHz and below), which are characteristic of the main signal in the initial portion of the JASON trace, are in excellent agreement with the moment derived by STEIN and OKAL (2005). Furthermore, all M_{TSU} measurements suggest $M_0 \geq 7 \times 10^{28}$ dyn-cm, is significantly larger than the *ad hoc* threshold ($M_0 = 5 \times 10^{28}$ dyn-cm) for generation of a tsunami posing substantial risk in the far field.

In view of the large number of approximations made, both in the definition of the M_{TSU} algorithm, and more importantly in its application to the JASON profile, we regard the ability of M_{TSU} to recover an estimate of the seismic moment of the Sumatra earthquake within bounds emphasizing its tsunamigenic potential in the far field as nothing short of spectacular. However, the JASON profile sampled a path located primarily in or near the lobes of directivity of the rupture. Thus, the only dataset available to date for processing the M_{TSU} algorithm from a truly gigantic source with a source length greater than 1000 km was favorably located in this respect, and there remains the possibility that the algorithm would underestimate such sources if applied at an azimuth where the interference is highly destructive.

6. Discussion and Conclusion

We have shown that tsunameter records can be interpreted in terms of the seismic moment of the parent earthquake in the framework of a rigorous theory which justifies all terms in the expression of M_{TSU} including its locking constant. The summary of our results, presented in Figure 9, shows that

* For events 2, 3, 4, 5 and 7, the average value of the mean M_{TSU} computed at individual stations recovers the seismic moments within 0.12 logarithmic units.
* In most such cases, the performance of the instrument[s] located in the Gulf of Alaska is degraded, probably as a result of the passage of the wave trains over the Aleutian Islands and the Bering Sea continental shelf.

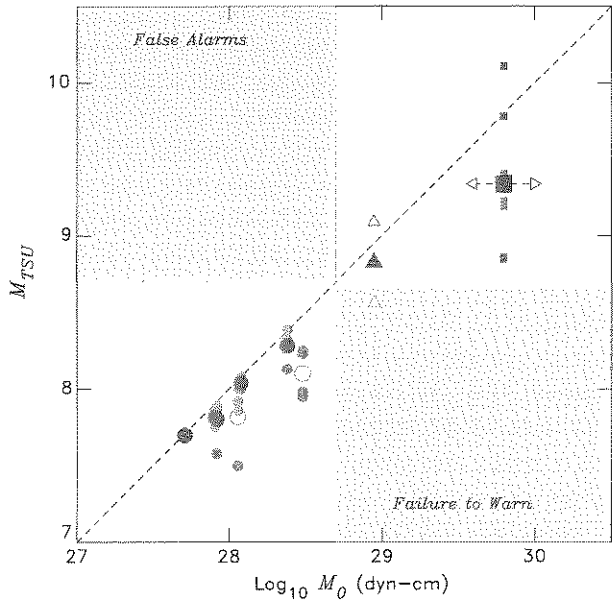

Figure 9

Summary of the performance of M_{TSU} for seven earthquakes, the 1946 simulation and the JASON trace of the 2004 Sumatra tsunami. This figure plots values of M_{TSU} obtained in the present study as a function of published seismic moment M_0. For the seven earthquakes recorded by tsunameters, the small shaded symbols are the mean values at each site, as listed in Table 1. For each event, their average over the various sites (shown in bold in Table 1) is plotted as a circle (events 1 and 5, showing deficiency in M_{TSU} use an open symbol; see text for discussion). The triangles relate to the 1946 simulation: open symbols show the mean at the two virtual gauges, the solid one the average of the latter. Sumatra data from the JASON trace are shown as squares: shaded symbols are values at the individual frequencies, the larger symbol their average; the horizontal double arrow shows the range of published moments, from the initial CMT solution to the normal mode study by STEIN and OKAL (2005). The two shaded regions illustrate domains of false alarms or failure to warn, using a threshold of 5×10^{28} dyn-cm for the source of a tsunami damaging in the far field. See text for details.

* In the case of event 1, the 1994 earthquake in the Kuriles, the deficiency of M_{TSU} *vs.* $\log_{10} M_0$ at the West Coast tsunameters (0.25 unit) is probably due to the singular depth and focal mechanism of the event, which does not involve interplate thrusting.
* Even for event 6, the 1995 Mexican earthquake, the source is adequately recovered at the West Coast sites, despite severe refraction around the American continent, in a geometry where the M_{TSU} algorithm would not be expected to work.
* The algorithm gives an adequate estimate of the moment of the great 2004 Sumatra earthquake from the JASON satellite altimeter dataset, even though the latter first had to be converted into a time series through a rather *ad hoc* procedure.

* Under the simplified assumption of a threshold of $M_0 \approx 5 \times 10^{28}$ dyn-cm for potential tsunami damage in the far field, the shaded quadrants in Figure 9 define schematically domains of false alarm (upper left) where the use of M_{TSU} would overestimate the event beyond the threshold, and of failure to warn (bottom right), where a deficient M_{TSU} would miss a potentially hazardous tsunami. It is noteworthy that only one point in the diagram falls into a shaded quadrant. In particular, all values measured on the JASON trace correctly predict a very large earthquake with $M_0 \geq 7 \times 10^{28}$ dyn-cm; measurements at the lowest frequencies ($f \leq 1$ mHz; average $M_{TSU} = 9.41$) define a truly gigantic event. The lone failure to warn is obtained at the West Coast virtual gauge for the 1946 simulation. This point represents an average of values featuring a regular decrease of M_{TSU} with increasing frequency (Fig. 3*f*), which expresses the destructive effect of source directivity at an unfavorable azimuth. However, M_{TSU} measured at the lowest frequencies ($f \leq 1$ mHz) does recover a correct estimate of the moment.

In conclusion, these observations suggest that M_{TSU} is a particularly robust algorithm, which, being fully justified from a theoretical standpoint, can be expected to provide reliable estimates of the seismic moment of large earthquakes, with measurements taken at or below 1 mHz giving particularly reliable estimates. The case of event 7 shows that it can work in the regional field, and thus become a contributor to real-time tsunami warning procedures.

Acknowledgments

This research was supported by the National Science Foundation, under Grant Number CMS-03-01054 to EAO.

References

ABE, K. (1981), *A new scale of tsunami magnitude, M_t*, Phys. Earth Planet. Inter. *27*, 194–205.

ALTERMAN, Z., JAROSCH, H., and PEKERIS, C.L. (1959), *Oscillations of the Earth*, Proc. Roy. Soc. Ser. *A*, *252*, 80–95.

ARTRU, J., DUČIĆ, V., KANAMORI, H., LOGNONNÉ, P., and MURAKAMI, M. (2005), *Ionospheric detection of gravity waves induced by tsunamis*, Geophys. J. Intl. *160*, 840–848.

BEN-MENAHEM, A., and ROSENMAN, M. (1972), *Amplitude patterns of tsunami waves from submarine earthquakes*, J. Geophys. Res. *77*, 3097–3128.

GELLER, R.J. (1976), *Scaling relations for earthquake source parameters and magnitudes*, Bull. Seismol. Soc. Amer. *66*, 1501–1523.

GILBERT, F. (1970), *Excitation of the normal modes of the Earth by earthquake sources*, Geophys. J. Roy. astr. Soc. *22*, 223–226.

GONZÁLEZ, F.I., BERNARD, E.N., MEINIG, C., EBLE, M.C., MOFJELD, H.O., and STALIN, S. (2005), *The NTHMP Tsunameter network*, Natural Hazards *35*, 25–39.

GUIBOURG, S., HEINRICH, P., and ROCHE, R. (1997), *Numerical modeling of the 1995 Chilean tsunami; impact on French Polynesia*, Geophys. Res. Letts. *24*, 775–778.

HANSON, J.A. and BOWMAN, J.R. (2005), *Dispersive and reflected tsunami signals from the 2004 Indian Ocean tsunami observed on hydrophones and seismic stations*, Geophys. Res. Letts. *32*(17), L17608, 5 pp.

KANAMORI, H. (1977), *The energy release in great earthquakes*, J. Geophys. Res. *82*, 2981–2987.

KANAMORI, H. and CIPAR, J.J. (1974), *Focal process of the great Chilean earthquake, May 22, 1960*, Phys. Earth Planet. Inter. *9*, 128–136.

LÓPEZ, A.M. and OKAL, E.A. (2006), *A seismological reassessment of the source of the 1946 Aleutian "tsunami" earthquake*, Geophys. J. Intl. *165*, 835–849.

LOVE, A.E.H., *Some Problems in Geodynamics* (Cambridge Univ. Press, 1911).

MANSINHA, L. and SMYLIE, D.E. (1971), *The displacement fields of inclined faults*, Bull. Seismol. Soc. Amer. *61*, 1433–1440.

OCCHIPINTI, G., LOGNONNÉ, P., KHERANI, A., and HÉBERT, H. (2005), *Modeling and detection of ionospheric perturbation associated with the Sumatra tsunami of December 26th, 2004*, Eos, Trans. Amer. Geophys. Un. *86*(52), U11A–0829 (abstract).

OKAL, E.A. (1982), *Mode-wave equivalence and other asymptotic problems in tsunami theory*, Phys. Earth Planet. Inter. *30*, 1–11.

OKAL, E.A. (1988), *Seismic parameters controlling far-field tsunami amplitudes: A review*, Natural Hazards *1*, 67–96.

OKAL, E.A. (1990), *Single forces and double-couples: A theoretical review of their relative efficiency for the excitation of seismic and tsunami waves*, J. Phys. Earth *38*, 445–474.

OKAL, E.A. (2003), *Normal mode energetics for far-field tsunamis generated by dislocations and landslides*, Pure Appl. Geophys. *160*, 2189–2221.

OKAL, E.A. and HÉBERT, H. (2007), *Far-field modeling of the 1946 Aleutian tsunami*, Geophys. J. Intl. in press.

OKAL, E.A. and TALANDIER, J. (1989), M_m: *A variable period mantle magnitude*, J. Geophys. Res. *94*, 4169–4193.

OKAL, E.A. and TALANDIER, J. (1991), *Single-station estimates of the seismic moment of the 1960 Chilean and 1964 Alaskan earthquakes, using the mantle magnitude* M_m, Pure Appl. Geophys. *136*, 103–126.

OKAL, E.A., PIATANESI, A., and HEINRICH, P. (1999), *Tsunami detection by satellite altimetry*, J. Geophys. Res. *104*, 599–615.

OKAL, E.A., SYNOLAKIS, C.E., FRYER, G.J., HEINRICH, P., BORRERO, J.C., RUSCHER, C., ARCAS, D., GUILLE, G., and ROUSSEAU, D. (2002), *A field survey of the 1946 Aleutian tsunami in the far field*, Seismol. Res. Letts. *73*, 490–503.

OKAL, E.A., TALANDIER, J., and REYMOND, D. (2007), *Quantification of hydrophone records of the 2004 Sumatra tsunami*, Pure Appl. Geophys. *164*, 309–323.

PELTIER, W.P. and HINES, C.O. (1976), *On a possible ionospheric technique for tsunami detection*, Geophys. J. Roy. astr. Soc. *46*, 669–706.

SAITO, M. (1967), *Excitation of free oscillations and surface waves by a point source in a vertically heterogeneous Earth*, J. Geophys. Res. *72*, 3689–3699.

SCHARROO, R., SMITH, W.H.F., TITOV, V.V., and ARCAS, D. (2005), *Observing the Indian Ocean tsunami with satellite altimetry*, Geophys. Res. Abstr. *7*, 230, (abstract).

SLADEN, A. and HÉBERT, H., *Inversion of satellite altimetry to recover the Sumatra 2004 earthquake slip distribution*, Eos, Trans. Amer. Geophys. Un. *86*(52), U22A–07, (2005) (abstract).

STEIN, S. and OKAL, E.A. (2005), *Size and speed of the Sumatra earthquake*, Nature *434*, 581–582.

SYNOLAKIS, C.E., *Tsunami and seiche*, In *Earthquake Engineering Handbook* (eds.) W.-F. Chen and C. Scawthron pp. 9_1–9_90, (CRC Press, Boca Raton, 2002).

TANIOKA, Y., RUFF, L.J., and SATAKE, K. (1995), *The great Kurile earthquake of October 4, 1994 tore the slab*, Geophys. Res. Letts. *22*, 1661–1664.

TITOV, V.V. and ARCAS, D. (2005), *Indian Ocean tsunami generation and propagation from modeling and observations*, Geol. Soc. Amer. Abstr. with Programs *37*(7), p.93, (abstract).

TITOV, V.V. and SYNOLAKIS, C.E. (1998), *Numerical modeling of tidal wave run-up*, J. Waterw. Port, Coastal and Ocean Eng. *124*, 157–171.

TITOV, V.V., GONZÁLEZ, F.I., BERNARD, E.N., EBLE, M.C., MOFJELD, H.O., NEWMAN, J.C., and VENTURATO, A.J. (2005), *Real-time tsunami forecasting: Challenges and solutions*, Natural Hazards *35*, 41–58.

TSAI, V.C., NETTLES, M., EKSTRÖM, G., and DZIEWOŃSKI, A.M. (2005), *Multiple CMT source analysis of the 2004 Sumatra earthquake*, Geophys. Res. Letts. *32*(17), L17304, 4 pp.

WARD, S.N. (1980), *Relationships of tsunami generation and an earthquake source*, J. Phys. Earth *28*, 441–474.

WARD, S.N. (1981), *On tsunami nucleation: I. A point source*, J. Geophys. Res. *86*, 7895–7900.

WARD, S.N. (1982a), *On tsunami nucleation: II. An instantaneous modulated line source*, Phys. Earth Planet. Inter. *27*, 273–285.

WARD, S.N. (1982b), *Earthquake mechanism and tsunami generation: the Kurile Islands event of October 13, 1963*, Bull. Seismol. Soc. Amer. *72*, 759–777.

WEAVER, P.F., YUEN, P.C., PRÖLSS, G.W., and FURUMOTO, A.S. (1970), *Acoustic coupling into the ionosphere from seismic waves of the earthquake at Kurile Islands on August 11, 1969*, Nature *226*, 1239–1241.

YEH, H., TITOV, V.V., GUSIAKOV, V., PELINOVSKY, E., KHRAMUSHIN, V., and KAISTRENKO, V. (1995), *The 1994 Shikotan earthquake tsunamis*, Pure Appl. Geophys. *144*, 855–874.

(Received January 7, 2006, accepted May 6, 2006)